

# Operational parameters affecting the performance of a mediator-less microbial fuel cell

Geun-Cheol Gil, In-Seop Chang, Byung Hong Kim\*, Mia Kim, Jae-Kyung Jang, Hyung Soo Park<sup>1</sup>, Hyung Joo Kim<sup>2</sup>

Water Environment Research Center, Korea Institute of Science and Technology, 39-1 Hawolgok, Sungpook, Seoul 136-791, South Korea

Received 1 October 2001; received in revised form 22 February 2002; accepted 28 May 2002

## Abstract

A mediator-less microbial fuel cell was optimized in terms of various operating conditions. Current generation was dependent on several factors such as pH, resistance, electrolyte used, and dissolved oxygen concentration in the cathode compartment. The highest current was generated at pH 7. Under the operating conditions, the resistance was the rate-determining factor at over 500  $\Omega$ . With resistance lower than 500  $\Omega$ , proton transfer and dissolved oxygen (DO) supply limited the cathode reaction. A high strength buffer reduced the proton limitation to some extent. The DO concentration was around 6 mg l<sup>-1</sup> at the DO limited condition. The fact that oxygen limitation was observed at high DO concentration is believed to be due to the poor oxygen reducing activity of the electrode used, graphite. The current showed linear relationship with the fuel added at low concentration, and the electronic charge was well correlated with substrate concentration from up to 400 mg l<sup>-1</sup> of COD<sub>cr</sub>. The microbial fuel cell might be used as a biochemical oxygen demand (BOD) sensor.

© 2002 Elsevier Science B.V. All rights reserved.

**Keywords:** Mediator-less; Microbial fuel cell; Biochemical oxygen demand sensor; Electrochemically active bacteria

## 1. Introduction

A microbial fuel cell is a device that converts chemical energy to electrical energy with the aid of the catalytic reaction of microorganisms (Allen and Bennetto, 1993; Kim et al., 1999b; Stirling et al., 1983; Rawson and Willmer, 1989; Suzuki et al., 1978; Wingard et al., 1982). A microbial fuel cell consists of anode and cathode compartments separated by a cation specific membrane. Microbes in the anode compartment oxidize fuel (electron donor) generating electrons and protons. Electrons are transferred to the cathode compartment through the circuit, and the protons through the membrane. Elec-

trons and protons are consumed in the cathode compartment reducing oxygen to water. Since most microbial cells are electrochemically inactive, electron transfer from microbial cells to the electrode is facilitated by the help of mediators such as thionine, methyl viologen, humic acid, and so on (Delaney et al., 1984; Lithgow et al., 1986). Since most of the mediators are expensive and toxic, a microbial fuel cell employing mediator has not been commercialized.

It has been shown that an Fe(III)-reducer, *Shewanella putrefaciens* is electrochemically active and can be used as a catalyst in a mediator-less microbial fuel cell (Kim et al., 1999a,c, 2002b). In addition, a fuel cell was used to enrich electrochemically active bacteria using wastewater from a starch processing factory as the electron donor and with activated sludge as the bacterial source (Kim et al., 2002a). An electrochemically active bacterium was isolated from the mediator-less microbial fuel cell, which has been operated for over 3 years using wastewater from a starch processing plant (Park et al., 2001).

\* Corresponding author. Tel.: +82-2-958-5831; fax: +82-2-958-5839

E-mail address: [bhkim@kist.re.kr](mailto:bhkim@kist.re.kr) (B.H. Kim).

<sup>1</sup> Present address: R&D Centre, Samsung Engineering Co. 39-3, Songbok-Ri, Suji-Eup, Yongin-City, Kyonggi-Do, 449-844, South Korea.

<sup>2</sup> Present address: Korea BioSystems Co., 39-1 Hawolgok, Sungpook, Seoul 136-791, South Korea.

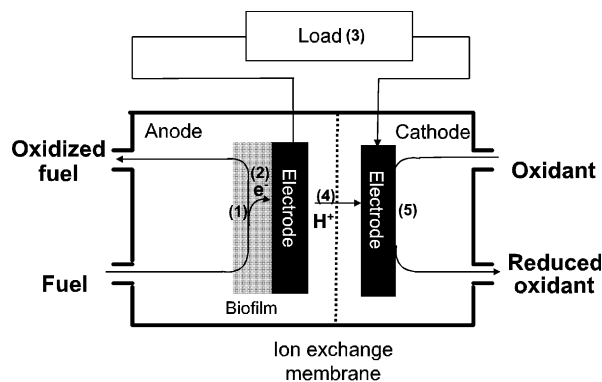


Fig. 1. Possible rate-limiting steps in a mediator-less microbial fuel cell. (1) Oxidation of fuel, (2) electron transfer from the microbial cells to the electrode, (3) electric load in the circuit, (4) Proton supply into the cathode compartment, and (5) Oxygen supply and reduction at the cathode.

The performance of a microbial fuel cell can be influenced by several factors. They are the rates of fuel oxidation and electron transfer to the electrode by the microbes, the resistance of the circuit, proton transport to the cathode through the membrane, and oxygen supply and reduction in the cathode (Fig. 1). In this study, a mediator-less microbial fuel cell having been operated for over 3 years was used to optimize the conditions listed above. Electron microscopic observation showed that the anode of the fuel cell enriched in a similar way was heavily inhabited by microbial communities consisting of thick biofilm at the surface of the electrode and microbial clumps loosely associated with the electrode (Kim et al., 2002a). Consistent coulomb yield was obtained under given operational conditions after the initial enrichment procedure for about 5 weeks. Rate-limiting steps of the mediator-less microbial fuel cell were considered and determined for each step.

## 2. Materials and methods

### 2.1. Wastewater and chemicals

Wastewater was collected from a starch processing plant (Samyang Genex Co., Korea). The chemical oxygen demand (COD chromate) of the wastewater was around  $1700 \text{ mg l}^{-1}$ . It was diluted using distilled water or 50 mM phosphate buffer (pH 7.0) containing 100 mM NaCl to a designated concentration before fed into the anode compartment as fuel.

### 2.2. Microbial fuel cell system

Three mediator-less microbial fuel cells enriched for over 3 years (Kim et al., 2002a) were used in this study. The anode and cathode compartments (working volume of 25 ml each) were separated by cation exchange

membrane (Nafion<sup>®</sup>, Dupont Co., USA). Graphite felt ( $50 \times 50 \times 3 \text{ mm}^3$ , GF series, Electro-synthesis Co., USA) was used as electrodes with platinum wire connecting them through resistance and a multimeter. Injection ports were installed in each compartment of the fuel cell. The experimental set-up is shown in Fig. 2.

The anode compartment was kept anoxic by purging nitrogen gas. Air was purged into the cathode compartment in order to supply oxygen needed for the electrochemical reaction. The gassing rate to each compartment was  $10 \text{ ml min}^{-1}$ . The cathode compartment contained 50 mM phosphate buffer (pH 7.0) with 100 mM NaCl as the electrolyte, and the anode compartment wastewater diluted with the electrolyte. The microbial fuel cells were placed in a temperature-controlled chamber. The resistance of  $10 \Omega$  was selected by resistance box. Optimization was made varying these standard conditions.

### 2.3. Dissolved oxygen (DO) monitoring system

When an oxygen electrode was placed in the cathode compartment to monitor DO, the current could not be measured probably due to the interference due to the high potential used in the oxygen electrode. To avoid this problem, DO was measured in a separate vial which received effluent from the cathode compartment continuously. Electrolyte was aerated in a separate chamber for over 6 hours before fed continuously into the cathode compartment. The effluent from cathode compartment was transferred to a continuously stirred vial that is equipped with a DO probe (Orion Co., UK) to monitor DO concentration of the effluent (Fig. 2). The vial was kept free of gas-phase to avoid changes in DO by diffusion. The working volume of the vial was 30 ml which is relatively large compared with the normal flow rate of  $24 \text{ ml h}^{-1}$  for the real time monitoring of DO, but the trend in DO change could be followed mainly due to the slow reaction. Data from DO meter was transferred into computer via RS-232 communication cable.

### 2.4. Instrumentation and analyses

The potential between anode and cathode was measured using a multimeter (Keithly Co., USA) and recorded every 5 minutes through a data acquisition system (Testpoint<sup>®</sup>, Capital Equipment Co., USA). The measured potential was converted to current according to the relationship of potential = current  $\times$  resistance. Coulomb, which is expressed as current  $\times$  time was calculated by integrating the current over the time from the start point of experiment to the time where current was decreased to 5% of maximum current. All experiments were conducted using 3 separate microbial fuel cells, and results were presented as average values or

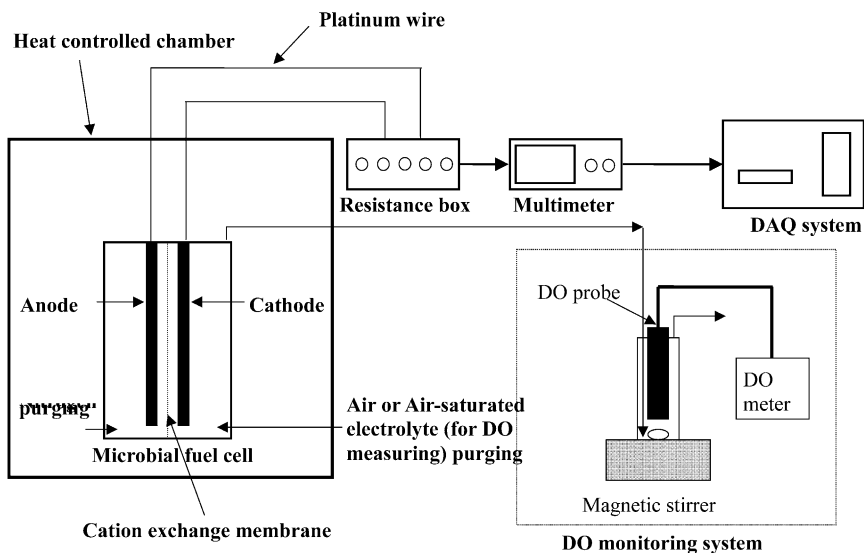


Fig. 2. Schematic diagram of the mediator-less microbial fuel cell with dissolved oxygen monitoring system using DO meter.

a typical result. Chemical oxygen demand (COD chromate) was measured by closed reflux titrimetric method using chromate as the oxidant (Andrew et al., 1995).

### 3. Results

#### 3.1. pH of the anode compartment

The anode content had been completely replaced with wastewater diluted with distilled water (COD value of  $400 \text{ mg l}^{-1}$ ) of varying pH from 5 to 9 before potential was recorded with  $1000 \Omega$  resistance (Fig. 3). As shown in the figure, the highest current was observed between pH 7 and 8 and the values were lower at pH 9 and below

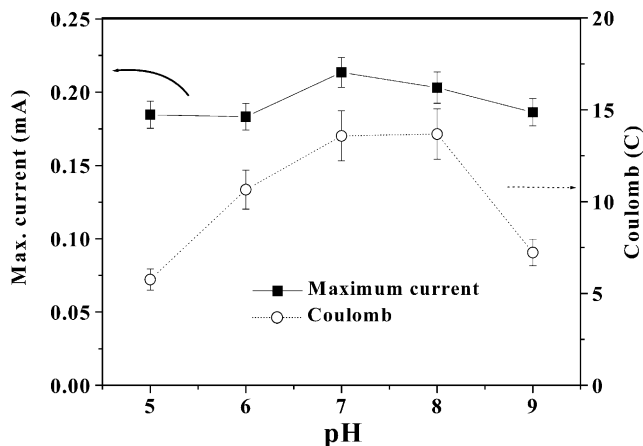


Fig. 3. Effects of pH on the performance of the microbial fuel cell. The fuel cells were operated at  $37^\circ \text{C}$  using a resistance of  $1000 \Omega$ . Wastewater was diluted using electrolyte containing  $50 \text{ mM}$  phosphate and the pH was adjusted. The anode and cathode compartments were gassed with  $\text{N}_2$  and air, respectively, at the rate of  $10 \text{ ml min}^{-1}$ . Wastewater with  $\text{COD}_{\text{cr}}$  of  $400 \text{ mg l}^{-1}$  was used for each experiment.

6. These results show that the microbial activity is slower at sub-optimal pH than at optimal pH. Coulombic output showed a similar trend but the differences were more significant than current. Low value at pH 9.0 might be due to poor proton transfer at the reduced proton concentration gradient across the membrane.

#### 3.2. Resistance

The fuel cells were operated with different resistance across the anode and cathode using wastewater with COD value of  $400 \text{ mg l}^{-1}$ . It was observed that the lower the resistance the higher the current (Fig. 4A). With resistance over  $500 \Omega$  a low-level current was steadily maintained for over 30 h. However, at low resistance of 10 and  $100 \Omega$ , the current reached the maximum values immediately after the fuel supply, and decreased rapidly with two shoulders. These results show that the resistance becomes the rate-limiting step (step 3 in Fig. 1) in the current generation at over  $500 \Omega$ , whilst electron consumption rate at the cathode is lower than transfer rate with a resistance lower than  $200 \Omega$ . This might be due to limited supply of proton or oxygen (steps 4 and 5 in Fig. 1).

Fig. 4B shows that the lower the resistance the higher the coulomb yield. The differences in coulomb yield means that some electrons are consumed by (a) mechanism(s) other than the cathode reaction. At this point it is not known how this is possible. It is plausible that under the conditions of limited electron disposal through the circuit with a high resistance, the electrons are consumed in the anode to reduce other electron acceptors such as sulfate and nitrate, or oxygen diffused through the membrane and the sampling ports. When the microbial fuel cells were operated without nitrogen gassing through the anode compartment, lower coulomb was

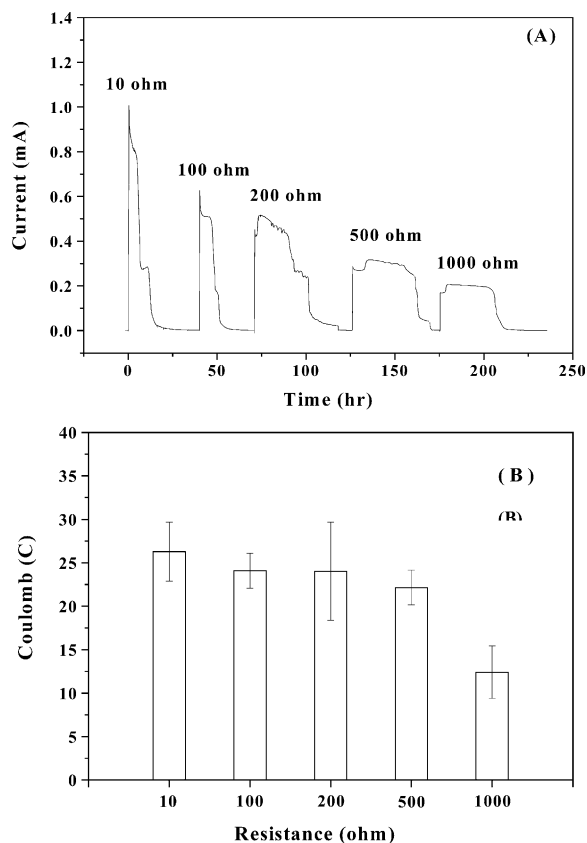


Fig. 4. Current generation (A) and coulomb (B) from the microbial fuel cells with different resistance. Resistance was varied from 10 to 1000  $\Omega$ , and pH of wastewater was adjusted to 7. The other experimental conditions were same as in Fig. 3.

obtained than with the nitrogen gassing. BOD values decreased gradually in the anode compartment disconnected from the cathode at a lower rate than in the connected one (data not shown).

### 3.3. Electrolyte

The microbial fuel cells were operated using wastewater diluted using different salt solutions to COD value of 100 ppm. Phosphate buffer (50 mM, pH 7.0) with 100 mM NaCl was used as the control to determine the effects of phosphate buffer and NaCl. The same salt solutions were used as the cathode electrolyte. As shown in Fig. 5, the highest current was generated from the control experiment which employed phosphate buffer with NaCl as the electrolyte followed by phosphate buffer alone and distilled water. The lowest current and coulomb were observed from the fuel cell with NaCl solution alone.

Another set of experiments were performed using 400 ppm wastewater diluted with distilled water to measure pH changes, which was compared to that of the control experiment using 50 mM phosphate buffer (pH 7.0) containing 100 mM NaCl (Fig. 6). In the control

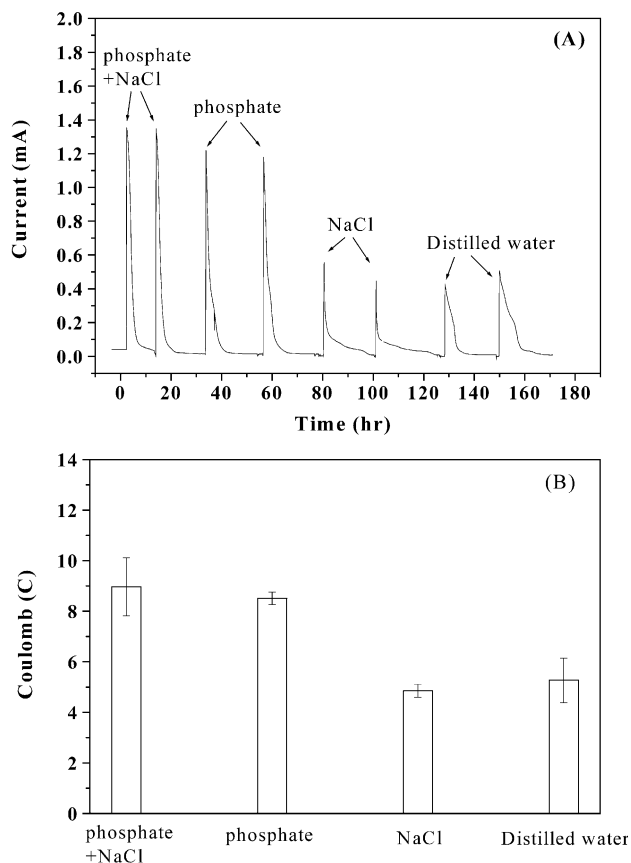


Fig. 5. Effects of electrolyte on the performance of the microbial fuel cell. (A) Current vs. time, and (B) Coulomb vs. electrolyte. The microbial fuel cells were operated with a resistance of 10  $\Omega$  under similar conditions as in Fig. 3. The wastewater was diluted to COD value of 100  $\text{mg l}^{-1}$  with electrolyte indicated in the figure.

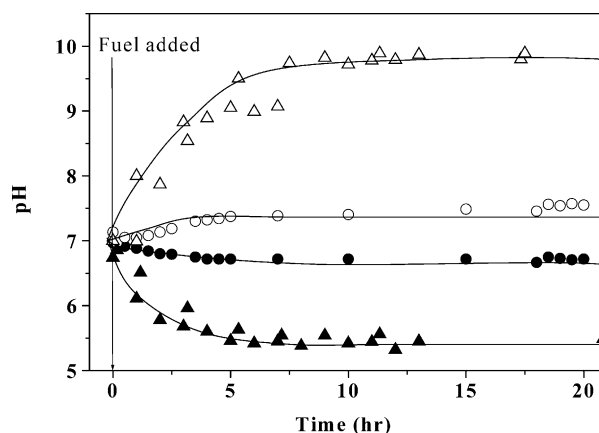


Fig. 6. Trend of pH changes in a microbial fuel cell using non-buffered electrolyte. The experimental conditions were similar as in Fig. 5.  $\circ$ ,  $\bullet$ , with phosphate buffer containing 100 mM NaCl;  $\square$ ,  $\blacktriangle$ : with distilled water. (Open symbols: cathode, closed symbols: anode.)

experiment pH changed less than 0.5 units both in cathode and anode after the fuel had been added, whilst the pH changes in the fuel cell without buffer were significantly higher than the control experiment. The pH

of the cathode compartment increased gradually up to over 9.5 after the supply of fuel, and that of anode compartment decreased to 5.4. These results show that proton transport through the membrane is slower than its production rate in the anode and its consumption rate in the cathode compartments, and that buffer can compensate the slow proton transport rate. Since the microbial fuel cell showed its optimum pH at neutral (Fig. 2), buffer is needed not only for the optimum microbial activities, but also to compensate the slow proton transport rate through the membrane.

Another set of experiments were conducted using 100mM phosphate buffer (pH 7.0) with 100 mM NaCl and the current generation pattern was compared to the control experiment (Fig. 7). The current decreased less rapidly in the experiment with 100 mM buffer than the control after the initial increase with the fuel supply. This result shows that the rapid decrease in current before the first shoulder is due to the limited proton supply.

#### 3.4. Aeration into the cathode compartment

Microbial fuel cells operated with aeration rate into the cathode compartment varied from 10 to 200 ml min<sup>-1</sup>. The anode compartment was purged by nitrogen at the same flow rate as the aeration rate to the cathode compartment. Fig. 8 shows that the maximum current increased as the aeration rate was increased up to 100 ml min<sup>-1</sup>. At the aeration rate of 200 ml min<sup>-1</sup>, current and coulomb were lower than those at 100 ml min<sup>-1</sup>. These results show that sufficient oxygen can be supplied at the aeration rate around 100 ml min<sup>-1</sup>. The poor performance of the microbial fuel cell at high gassing rate might be due to the shear force disturbing microbes immobilized onto the anode.

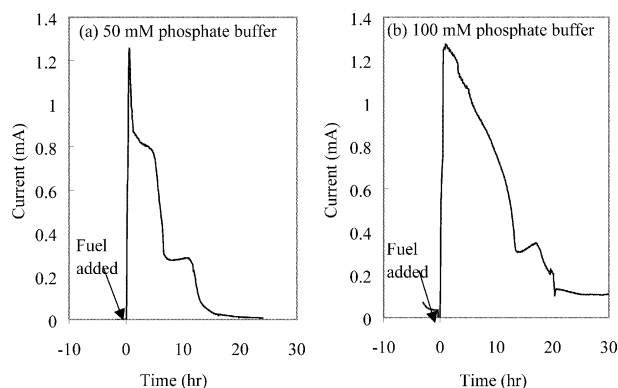


Fig. 7. Current patterns with different concentration of buffer as the electrolyte. The microbial fuel cells were fed with wastewater with COD of 400 ppm containing 50 mM (A) or 100 mM (B) phosphate buffer containing 100 mM NaCl, respectively. The fuel cells were operated at pH 7.0, temperature 37 °C, resistance 10 Ω. N<sub>2</sub> and air were gassed through the anode and cathode compartments, respectively, at the rate of 10 ml min<sup>-1</sup>.

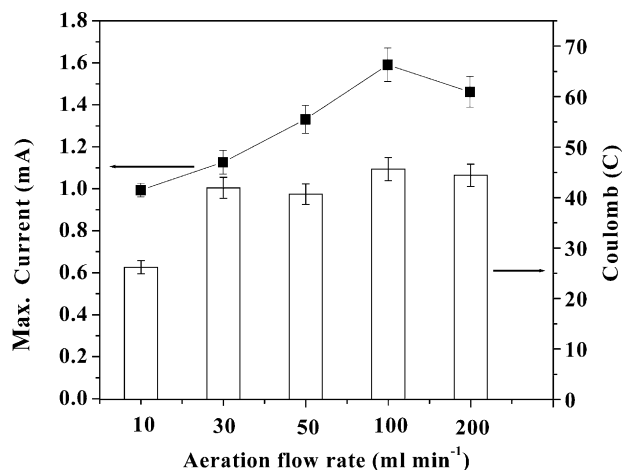


Fig. 8. Effects of the aeration rate on the performance of the microbial fuel cell. The cathode compartment was aerated at the rate indicated in the figure, and the anode gassed with N<sub>2</sub> at the same rate as the cathode aeration rate. The fuel cells were operated at 37 °C and pH 7 using a resistance of 10 Ω. Wastewater was diluted using electrolyte containing 50 mM phosphate with 100 mM NaCl to make 400 mg l<sup>-1</sup> COD<sub>cr</sub>.

#### 3.5. Dissolved oxygen monitoring of cathode compartment

The microbial cells were operated with feeding air-saturated electrolyte continuously to the cathode compartment instead of aeration to monitor dissolved oxygen. Starch wastewater with the COD value of 400 mg l<sup>-1</sup> was used as fuel, and the current and DO concentration with different electrolyte flow rates were compared (Fig. 9). The current generation pattern was different from those of aerated microbial fuel cell. The initial maximum current was much lower than the aerated operation and only a big shoulder was observed instead of two shoulders. This result shows that air-saturated electrolyte cannot supply enough oxygen to reach the proton limited condition.

After the initial jump, current dropped to around 0.6 mA in the cell with high electrolyte flow (90 ml h<sup>-1</sup>) and to around 0.4 mA in that with low electrolyte flow rate (24 ml h<sup>-1</sup>). After these rapid drops, the current decreased slowly before it dropped to the background level probably due to the depletion of the fuel. With the initial rapid increase in current, the DO level dropped to 5.5 mg l<sup>-1</sup> in the cathode compartment which received air saturated electrolyte at 90 ml h<sup>-1</sup>, to 6.0 mg l<sup>-1</sup> in the cathode compartment at 24 ml h<sup>-1</sup>. After the initial drop DO increased steadily before increasing rapidly with the depletion of fuel. This decrease in current and increase in DO might be caused by other factor(s) limiting the cathode reaction. Similar results were obtained from the fuel cells operated using a 100 mM phosphate buffer (instead of usual 50 mM, pH 7.0) with 100 mM NaCl (data not shown) showing that proton in the cathode compartment is not limiting. Another set of

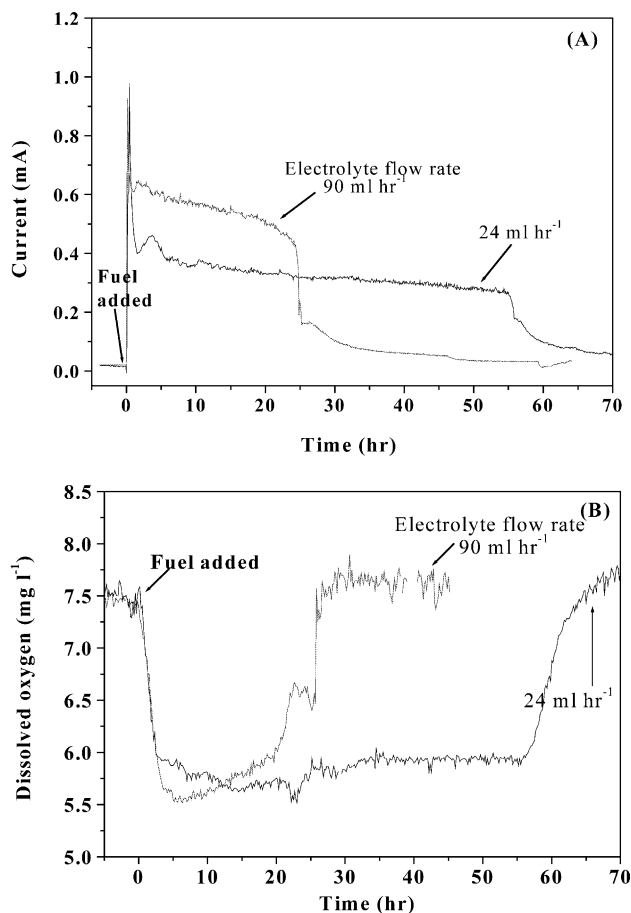


Fig. 9. Current (A) and of dissolved oxygen concentration in the cathode compartment (B) of microbial fuel cells, cathodes of which were fed continuously with air-saturated electrolyte at different rate. Air-saturated 50 mM phosphate buffer containing 100 mM NaCl was continuously fed into cathode compartment at the rate of 90 or 24 ml h<sup>-1</sup>, respectively. Wastewater with a COD value of 400 mg l<sup>-1</sup> was used. The fuel cells were operated at the optimum conditions; pH 7.0, temperature 37 °C, resistance 10 Ω, and N<sub>2</sub> gassing rate of 100 ml min<sup>-1</sup> into the anode compartment.

experiments was set up to test the effect of aeration on the current generation and on DO. A similar trend was observed when the cathode compartment was fed with electrolyte at the flow rate of 90 ml h<sup>-1</sup>. When the cathode compartment was aerated, the current increased sharply, and so did DO slowly (Fig. 10). When the aeration was stopped the current decreased to the original level, whilst the decrease in DO was less significant. The high DO value after the aeration had been stopped was due to the air bubbles in the oxygen electrode chamber. These results show that DO is the major limiting factor for the operation of a microbial fuel cell where graphite is used as the electrode.

The maximum current obtained in Fig. 10 was around 1.7 mA, which is higher than those obtained in the control experiments (Figs. 4A and 7). This can be explained as better proton compensation through the continuous flow of the buffer solution.

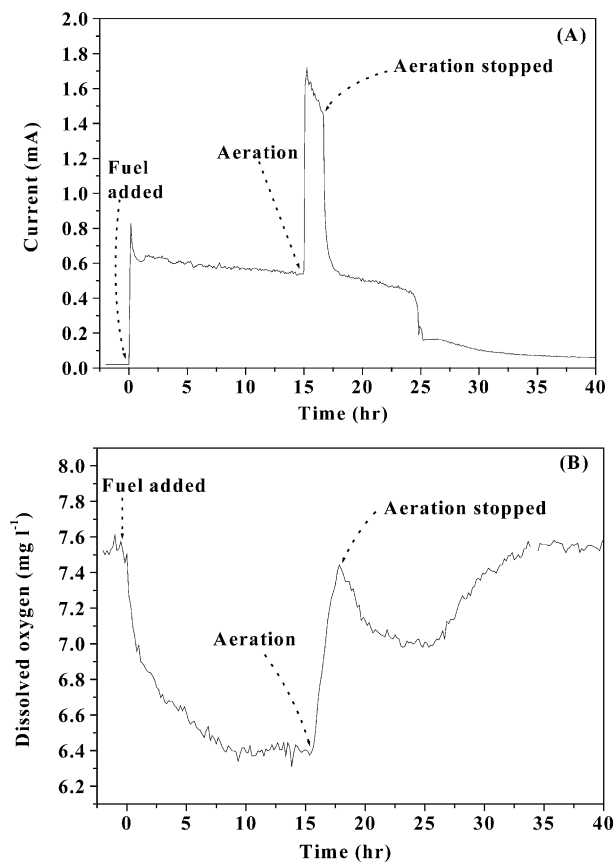


Fig. 10. The effects of aeration into the cathode compartment receiving air-saturated electrolyte continuously on current (A) and dissolved oxygen concentration in the cathode compartment (B). A microbial fuel cell was operated in a similar way as in Fig. 9 with the electrolyte flow rate of 90 ml h<sup>-1</sup>. During the experiment, air was gassed through the cathode compartment at the point indicated in the figure at the rate of 100 ml min<sup>-1</sup>.

### 3.6. Fuel concentration and current generation

The microbial fuel cells were run using different concentrations of wastewater to determine the correlation between the fuel concentration and the maximum current. As shown in Fig. 11A the maximum current increased with the wastewater concentration up to 50 mg l<sup>-1</sup>. The coulomb increased linearly up to 400 mg l<sup>-1</sup> (Fig. 11B). These results show that the mediator-less microbial fuel cell can be used as a biosensor to measure the strength of wastewater.

## 4. Discussion

A microbial fuel cell has great potential as a wastewater treatment process since organic contaminants are converted into electricity with the concomitant reduction of the excess sludge production. It has been shown that a mediator-less microbial fuel cell can be constructed using electrochemically active microbial enrich-

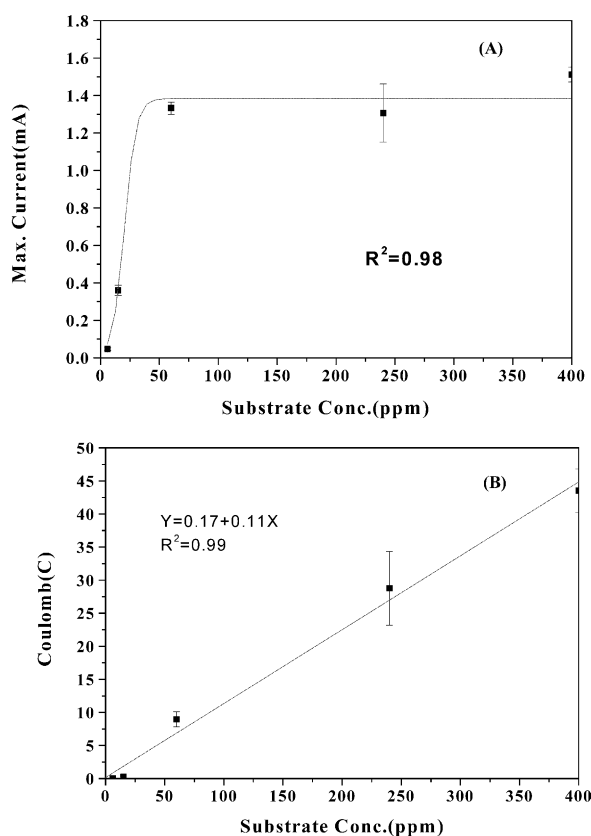
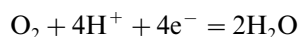


Fig. 11. Relationship between fuel concentration and the maximum current (A), and coulomb (B) from the microbial fuel cell. The fuel cells were fed with diluted wastewater diluted to the concentration indicated in the figure using 50 mM phosphate buffer (pH 7.0) containing 100mM NaCl. The fuel cells were operated at pH 7.0, temperature 37 °C, resistance 10  $\Omega$ , and  $N_2$  and air were gassed at the rate of 100 ml  $min^{-1}$ .

ment culture (Kim et al., 2002a). In the anode compartment of a microbial fuel cell, the fuel is oxidized to carbon dioxide transferring electrons to the electrode and liberating protons into the aqueous phase. Dioxygen is reduced to water in the cathode compartment with electron transferred through the circuit and proton through the membrane according to the following equation:



As shown in Fig. 1 there can be several rate-limiting steps in the current generation by a microbial fuel cell. Since microbial fuel cells used in this study were enriched and operated for over 3 years, it is assumed that the microbial consortium in the anode compartment is in its maximum activity in terms of fuel oxidation (step 1) and electron transfer to the electrode (step 2). Based on this assumption studies were made to optimize steps 3–5.

At low resistance the microbial fuel cell generated higher current which dropped rapidly with shoulders probably due to rate-limiting factors such as proton

transfer and oxygen supply (Fig. 4A). The initial jump in current is thought to be possible with proton and oxygen accumulated during the starvation period. The first shoulder in the current generation from the fuel cell operated with 10 and 100  $\Omega$  disappeared when 100 mM phosphate was used as the electrolyte (Fig. 7), and when the air-saturated electrolyte was used instead of aeration (Figs. 9 and 10). From these results, it is concluded that the first shoulder is due to the proton limitation, and the second due to oxygen limitation.

When the microbial fuel cells were operated without phosphate buffer, the maximum current generated was much lower than with buffer (Fig. 5) with the pH changes to over 9.5 in the cathode compartment and to 5.4 in the anode compartment (Fig. 6). These results show that the proton permeability through the membrane is too poor for the efficient operation of the microbial fuel cell. Under the proton transfer limited conditions, the microbial activity and the electron transfer to the electrode in the anode compartment can be reduced due to the pH change (Fig. 3) in addition to the slow cathode reaction due to limited supply of proton. A non-compartmentalized fuel cell should be developed to overcome this problem (Katz et al., 1999).

The microbial fuel cell could be operated under oxygen limited condition with the continuous air-saturated electrolyte instead of aeration (Figs. 9 and 10). At this condition the DO concentration was between 5.5 and 6.4  $mg\ l^{-1}$ . These figures are very high as a limiting DO concentration probably due to poor catalytic activity of graphite reducing dioxygen. This problem can be solved by modification of the electrode surface (Palmore and Kim, 1999; Tsujimura et al., 2001).

The lowest resistance tested that limited the overall performance of the microbial fuel cell was 500  $\Omega$ . With this resistance the fuel cell generated a maximum current of 0.3 mA for about 30 h. This figure can be used to calculate dioxygen and proton consumption rates, which are the performance characteristics of the fuel cell under the operation conditions. Current (A) is expressed as  $C\ s^{-1}$ , and 0.3 mA is  $0.3\ mC\ s^{-1}$ , which is  $1080\ mC\ h^{-1}$ . By dividing this figure with Faraday constant ( $96,487\ C\ mol^{-1}$ ), the average electron consumption rate in the cathode compartment can be calculated;  $10,803\ mC\ h^{-1}/96,487\ C\ mol^{-1} \cong 11.19\ \mu\ electron\ equivalent\ h^{-1}$ . Under this condition the amount of dioxygen and proton consumed were calculated as 2.80 and 11.19  $\mu\ mol\ h^{-1}$ , respectively. These figures should be increased for the better performance of the microbial fuel cell by increasing the membrane permeability and by improving the catalytic activity of the cathode.

The maximum current obtained was 1.7 mA (Fig. 10a). This figure was used to calculate the organic contaminant consumed in a similar way. The electron consumption rate was  $63.43\ \mu\ electron\ equivalent\ h^{-1}$ ,

which can be converted to oxygen consumption rate of  $15.86 \mu\text{mol O}_2 \text{ h}^{-1}$  or  $0.51 \text{ mg l}^{-1} \text{ BOD removed h}^{-1}$ . Since the anode volume is 25 ml, the overall BOD removal rate can be  $489.6 \text{ mg BOD l}^{-1} \text{ day}^{-1}$ . These figures can be converted to  $0.68 \text{ A}$  and  $204 \text{ mg l}^{-1} \text{ BOD removed h}^{-1} \text{ m}^{-2}$  electrode surface, since the microbial fuel cell employed an electrode with a surface area of  $25 \text{ cm}^2$ . Higher BOD removal rate might be possible by increasing the cathode reaction through improvements in proton transfer and oxygen supply, and in the catalytic activity of the cathode.

The maximum current generated was related to the amount of fuel added at low concentrations lower than  $50 \text{ mg l}^{-1} \text{ COD}$ , while the coulomb values were linearly increased with the fuel concentration (Fig. 11). This device can be used as a biochemical oxygen demand (BOD) sensor.

## 5. Conclusion

The effects of operational conditions of a microbial fuel cell were tested and optimized for the best performance of a mediator-less microbial fuel cell. The optimal pH was 7. The resistance higher than  $500 \Omega$  was the rate-determining factor by limiting electron flow from anode to cathode. At the resistance lower than  $200 \Omega$ , proton and oxygen supplies to the cathode were limited. For the construction of an efficient microbial fuel cell, a non-compartmentalized fuel cell with an electrode having a high oxygen reducing activity should be developed. Since the concentration of fuel determines the amount of electricity generation from the fuel cell, the device can be used as a BOD sensor.

## Acknowledgements

This study was supported partly by the Ministry of Science and Technology of Korea National Research Laboratory Programme.

## References

Allen, R.M., Bennetto, H.P., 1993. Microbial fuel-cells: electricity production from carbohydrates. *Appl. Biochem. Biotechnol.* 39/40, 27–40.

Andrew, D.E., Clescenri, L.S., Breenberg, A.E., 1995. Standard Method for the Examination of Water and Wastewater, 19th ed.. APHA, AWW, WEF, Washington, DC, USA, pp. 5–14.

Delaney, G.M., Bennetto, H.P., Mason, J.R., Roller, H.D., Stirling, J.L., Thurston, C.F., 1984. Electron transfer coupling in microbial fuel cells: 2. Performance of fuel cells containing selected microorganism–mediator–substrate combinations. *J. Chem. Technol. Biotechnol.* 34B, 13–27.

Katz, E., Willmer, I., Kotlyar, A.B., 1999. A non-compartmentalized glucose/ $\text{O}_2$  biofuel cell by bioengineered electrode surface. *J. Electroanal. Chem.* 479, 64–68.

Kim, B.H., Kim, H.J., Hyun, M.S., Park, D.H., 1999a. Direct electrode reaction of Fe(III)-reducing bacterium, *Shewanella putrefaciens*. *J. Microbiol. Biotechnol.* 9, 127–131.

Kim, B.H., Ikeda, T., Park, H.S., Kim, H.J., Hyun, M.S., Kano, K., Takagi, K., Tatsumi, H., 1999b. Electrochemical activity of an Fe(III)-reducing bacterium, *Shewanella putrefaciens* IR-1, in the presence of alternative electron acceptors. *Biotechnol. Technol.* 13, 475–478.

Kim, H.J., Hyun, M.S., Chang, I.S., Kim, B.H., 1999c. A microbial fuel cell type lactate biosensor using a metal-reducing bacterium, *Shewanella putrefaciens*. *J. Microbiol. Biotechnol.* 9 (3), 365–367.

Kim, B.H., Park, H.S., Kim, H.J., Hyun, M.S., Kim, G.T., Kim, M.A., 2002a. Enrichment of electrochemically active anaerobic bacteria using a fuel cell type electrochemical cell. *Appl. Environ. Microbiol.*, submitted for publication.

Kim, H.J., Park, H.S., Hyun, M.S., Chang, I.S., Kim, M.A., Kim, B.H., 2002b. A mediator-less microbial fuel cell using a metal reducing bacterium, *Shewanella putrefaciens*. *Enzyme Microbiol. Technol.* 30, 145–152.

Lithgow, A.M., Romero, L., Sanchez, I.C., Souto, F.A., Vega, C.A., 1986. Interception of electron-transport chain in bacteria with hydrophilic redox mediators. *J. Chem. Res. (S)*, 178–9.

Palmore, G.T.R., Kim, H.-H., 1999. Electro-enzymatic reduction of dioxygen to water in the cathode compartment of a biofuel cell. *J. Electroanal. Chem.* 464, 110–117.

Park, H.S., Kim, B.H., Kim, H.S., Kim, H.J., Kim, G.T., Kim, M., Chang, I.S., Park, Y.K., Chang, H.I., 2001. A novel electrochemically active and Fe(III) reducing bacterium phylogenetically related to *Clostridium butyricum* isolated from a bacterial fuel cell. *Anaerobe* 7, 297–306.

Rawson, D.M., Willmer, A.J., 1989. Whole-cell biosensors for environmental monitoring. *Biosens. Bioelectron.* 4, 299–311.

Stirling, J.L., Bennetto, H.P., Delaney, G.M., Mason, J.R., Roller, S.B., Tanaka, K., Thurston, C.F., 1983. Microbial fuel cells. *Biochem. Soc. Trans.* 11 (4), 451–453.

Suzuki, S., Karube, I., Matsunaga, T., 1978. Application of a biochemical fuel cell to wastewater. *Biotechnol. Bioeng. Symp.* 8, 501–511.

Tsujimura, S., Tatsumi, H., Ogawa, J., Shimizu, S., Kano, K., Ikeda, T., 2001. Bioelectrocatalytic reduction of dioxygen to water at neutral pH using bilirubin oxidase as an enzyme and 2,2'-azinobis (3-ethylbenzothiazolin-6-sulfonate) as an electron transfer mediator. *J. Electroanal. Chem.* 496, 69–75.

Wingard, L.B., Shaw, C.H., Castner, J.F., 1982. Bioelectrochemical fuel cells. *Enzyme Microb. Technol.* 4, 137–142.